# Development of a Constitutive Theory for Short Fiber Yams: Part III: Effects of Fiber Orientation and Bending Deformation

Ning Pan

*Textile Research Journal* 1993; 63; 565
DOI: 10.1177/004051759306301002

9. Johnson, G. C., Reactive Silicone Softeners, *Book AATCC Papers*, 250–255 (1977).
10. Joyner, M. M., Aminofunctional Polysiloxanes: A New Class of Softeners, *Text. Chem. Color.* **18**, 34–37 (1986).
11. Kissa, E., Repellent Finishes, in "Handbook of Fiber Science & Technology," vol. II, M. Lewin, and S. B. Sello, Eds., Marcel Dekker, Inc., NY, 1984, pp. 142–210.
12. Pawlenko, S., "Organosilicone Chemistry," Walter de Gruyter, NY, 1986, p. 186.
13. Plueddemann, E. P., "Silane Coupling Agents," 2nd ed., Plenum Press, NY, 1991, p. 64.
14. Polmanteer, K. E., Current Perspectives on Silicone Rubber Technology, *Rubber Chem. Tech.* **54**, 1051–1080 (1981).
15. Sabia, A. J., and Metzler, R. B., The Role of Silicones in Nonwoven Fabric Applications, *Nonwovens Ind.* **14**, 16–22 (1983).
16. Schuyten, H. A., Weaver, J. W., Reid, D., and Jurgens, J. F., Trimethylsilycellulose, *J. Am. Chem. Soc.* **70**, 1919–1920 (1948).
17. Shin, Y., Hollies, N. R. S., and Yeh, K., Polymerization-Crosslinking of Cotton Fibers for Superior Performance Properties, Part I, A Preliminary Study, *Textile Res. J.* **59**, 635–642 (1989).
18. Turner, J. D., Improving the DP Appearance of Cotton Fabrics with Additives and Aminofunctional Silicones, *Textile Chem. Color.* **20**, 36–38 (1988).
19. Warrick, E. L., Pierce, O. R., Polmanteer, K. E., and Saam, J. C., Silicone Elastomer Developments 1967–1977, *Rubber Chem. Tech.* **52** (3), 437–525 (1979).
20. Watt, J. A. C., Water-Repellent Treatment of Textiles with Silicones: Studies on the Mechanisms of Two Processes, *J. Textile Inst.* **48**, T175–T192 (1957).

*Manuscript received November 9, 1992; accepted February 5, 1993.*

# Development of a Constitutive Theory for Short Fiber Yarns

## Part III: Effects of Fiber Orientation and Bending Deformation

NING PAN

*Division of Textiles and Clothing, University of California, Davis, California 95616, U.S.A.*

ABSTRACT

This article deals with the effects of fiber orientation and bending deformation on staple yarn behavior. First, the effect of fiber orientation is shown by comparing yarn properties determined using three different fiber orientation cases. Then, for a given fiber orientation distribution, radial distributions of both tensile stress and lateral pressure along the yarn cross section are predicted. The fiber obliquity effect at high yarn twist levels is attributed more to fiber bending deformation. Finally a modified yarn model is proposed that produces predictions in close agreement with existing experimental results.

For any structural materials, the properties of whole systems depend on the properties of their constituent materials, their concentrations and orientations, and the interactions of these materials. Concentration is a measure of homogeneity or uniformity of the system, and is usually measured in terms of volume or weight fraction, whereas orientation represents the anisotropy of the structure and can be specified, for example, using a statistical density function. This principle certainly applies to the case of a staple yarn where the constituent

materials are staple fibers. In Parts I and II of this series [11, 12], we used the yarn fiber-volume fraction $V_f$, averaged over the yarn cross section because of the nonuniformity of the yarn structure, to specify fiber concentration. In addition, by assuming all fibers in the yarn are distributed randomly with the yarn surface helical angle as the upper limit, we were able to derive a probabilistic density function. In this paper, we further examine the effect of fiber orientation on yarn behavior.

Fibers in a yarn are not aligned in parallel with the yarn axis, but follow the curved loci due to the twisting effect. Fiber paths can be resolved into circumferential and radial components. When the radial position of fibers is constant, they are distributed on the surfaces of coaxial columns. This brings out the simplest theoretical description of fiber orientation, known as the ideal coaxial model, first proposed by Gégauff in 1907 in a French paper [4] and later developed independently by Platt in 1950 [13]. To a large extent this model is acceptable as a representation of the real filament yarn structure, since filament yarn is much more uniform in both fiber-volume fraction and fiber configuration within the yarn [14]. On the other hand, a description of the fiber paths in a staple yarn is extremely difficult, partly due to the variation of radial positions of fibers in the yarn. The discontinuity of fiber length in a staple yarn adds another dimension to the complexity of the problem. Change in fiber radial positions is better known as fiber migration, which occurs during the yarn spinning process through self-adjusting of the tension in individual fibers. With migration, all fibers are gripped at some points along their length, and the yarn as a whole has the necessary self-locking characteristic.

In order to analytically study the effect of fiber migration or fiber orientation, we need an effective way to define fiber paths within the yarn. There are two different approaches: the first one is based on a geometric analysis of fiber paths so as to build a geometric model for further analysis. One encounters some problems with this approach because of the complexity of fiber paths in a staple yarn.

The second approach is a statistical one. In a real staple yarn structure, the forms of orientation that fibers may assume can be rather complex. A mathematical description of an individual fiber path within a yarn is a formidable, perhaps even impossible, task. This brings us at once to the necessity of adopting a statistical point of view. Van Wyk [15] and Cox [2] were perhaps among the first to use the statistical method to describe fiber orientation in a fibrous structure. Several researchers [3, 6, 7, 8, 16, 1] followed in applying a statistical approach to tackle the problem of fibrous structures. Such statistical analyses provide an appropriate technique to deduce average effects over the total population of fibers; using this method, one can then determine the system response and properties.

One problem associated with the statistical method is the difficulty of determining the form of the density function for a particular case; there has not been a unified and effective way to derive such a function. Another problem is that statistical approaches reveal only the average behavior of the system. It is possible [9] that two systems with differently oriented components can lead to the same result statistically.

Another issue addressed in this paper relates to the influence of fiber bending deformation during yarn extension. In all previous yarn models, fibers are assumed to be ideally flexible, so that they have no bending stiffness. This is of course not true. When fibers are all oriented in angles with respect to the yarn axis, the axis coincides with the external loading direction in the tensile case. Bending deformation of fibers caused by this yarn axial tensile load is inevitable and most likely plays an important role in yarn deformation.

## The Statistical Approach

As we stated above, although the statistical treatment using a probabilistic distribution function of fiber orientation is usually a better option than the geometric analysis, the major difficulty comes from determining the probability density function for a specific case. For a fiber network, Cox [2] proposed that such a density function can be assumed to be the form of a Fourier series. The constants in the series depend on the specific structures. For simple and symmetrical orientations, the coefficients are either eliminated or determined without much difficulty. However, it becomes problematic for complex cases where asymmetrical terms exist. Because of the central limit theorem, another option is to apply the Gaussian function or its equivalent in the periodic case, the Moice function [10], to approximate the structure in question, provided the coefficients in the functions can be determined through (most probably) experimental approaches.

Yet for an axially symmetric structure like a yarn, its density function can be more conveniently estimated in terms of the angular coordinates of fibers. As illustrated in Part I, the azimuthal angles $\phi$ of the fibers in a yarn can be approximated as uniformly distributed in the range $0 \leq \phi \leq \pi$, so that the density function is independent of $\phi$. Moreover, the polar angles $\theta$ are in

fact the helix angles of fibers in the yarn, and $0 \leq \theta \leq q$, where $q$ is the yarn surface helix angle. In Parts I and II, we have assumed that all fibers in a yarn are oriented in a totally random manner with no preferred direction. The randomness of fiber orientation implies that the density function is independent of $\theta$ as well. Therefore, this density function has the form of

$$\Omega(\theta, \phi) \sin \theta = \Omega_0 \sin \theta \quad , \qquad (1)$$

where $\sin \theta$ is the Jacobian of the vector of the direction cosines corresponding to $\theta$ and $\phi$, and $\Omega_0$ is a constant whose value is determined using the normalization condition:

$$\Omega_0 = \frac{1}{\pi(1 - \cos q)} \quad . \qquad (2)$$

This function is applicable to the real staple yarn structure where random distribution is a close description of the actual fiber orientation.

Lee and Lee [9], on the other hand, proposed a relatively general way to derive the density function for a fiber structure. Suppose the partial sum of the length of the fiber segments whose orientation is between $\theta \sim \theta + d\theta$ and $\phi \sim \phi + d\phi$ is $dL$ in a fibrous structure of total fiber length $L$. Then the density function $\Omega(\theta, \phi)$ of fiber orientation in this structure can be defined as

$$\Omega(\theta, \phi) \sin \theta d\theta d\phi = \frac{dL}{L} \quad . \qquad (3)$$

By calculating the partial length $dL$ and the total fiber length $L$ in the system, Lee and Lee derived the density function for the ideal coaxial helix geometry as

$$\Omega(\theta, \phi) \sin \theta = \frac{2 \sin \theta}{\pi \tan^2 \theta \cos^3 q} \quad , \qquad (4)$$

where $q$ again is the surface helical angle of the yarn.

Using the function in Equation 4, we can obtain all the statistical factors in the analysis of Part I:

$$K_L = \frac{2(\cos q - \cos^2 q)}{\sin^2 q} \quad ,$$

$$K_T = \frac{2\left(\frac{\sin q}{\cos^2 q} - \ln\left(\frac{1 + \sin q}{\cos q}\right)\right)}{\pi \tan^2 q} \quad ,$$

$$M_{TT}{}^a = \frac{1}{2} + \frac{\ln \cos q}{\cos q} \quad ,$$

$$M_{12}{}^a = M_{21}{}^a = \frac{1}{\pi} + \frac{2 \ln \cos q}{\pi \tan^2 q} \quad ,$$

$$M_{LL}{}^a = \frac{-2 \ln \cos q}{\tan^2 q} \quad ,$$

$$M_{LT}{}^a = M_{TL}{}^a = \frac{4(\tan q - q)}{\pi \tan^2 q} \quad .$$

To compare the differences between the two density functions, let us consider the nonslipping case only for simplicity. Note also that among all the yarn properties predicted in Part I, the longitudinal tensile modulus $E_L$ is the most familiar, and perhaps the only yarn parameter that can be readily verified by existing experiments. For this reason, we select $E_L$ from Equation 72 of Part I,

$$E_L = \frac{V_f E_f \eta_l K_L{}^2}{M_{LL}{}^a} \quad , \qquad (5)$$

for comparison using the two different forms of density functions.

Actually, as Equation 5 shows, the only part of the longitudinal tensile modulus that is affected by the density function is reflected in the terms related to fiber orientation, *i.e.*, $\frac{K_L{}^2}{M_{LL}{}^a}$. We can call the density function defined in Equation 1 $f_1$ and that in Equation 4 $f_2$; the results of these two functions along with the result from the well known $\cos^2 q$ law (the ideal coaxial model) are provided in Figure 1. Unlike the result of the $\cos^2 q$ law, the curves of both density functions predict a significant effect of fiber obliquity only when the yarn surface helix angle becomes impractically high,

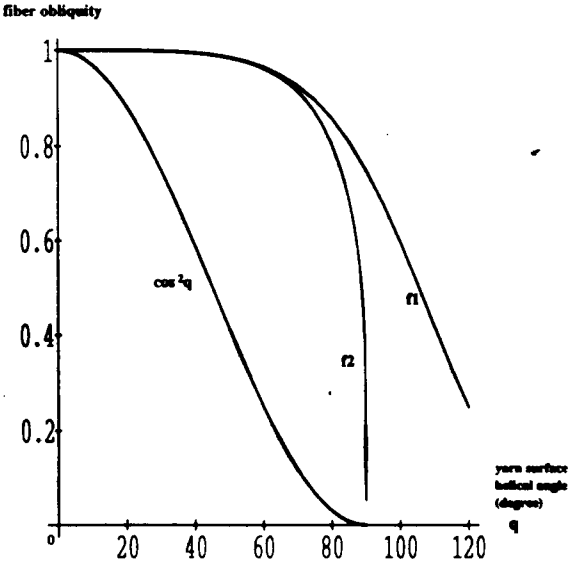


FIGURE 1. Fiber obliquity effect predicted by three fiber orientation models.

since according to reference 5 for filament yarns, the maximum possible value of $q$ cannot exceed 70.5 degrees. There are several options to modify the model: The first is to derive a better density function; the second is to adjust the range of the surface helix angle of staple yarns because it should be different from that of a filament yarn. Also, we need to determine other factors that may contribute to the fiber obliquity effect but have not been included in our analysis. We will explore these last two options in the later sections of this paper.

## Stress Distributions Along the Radial Positions of a Staple Yarn

In Part I of this study, we derived the tensile and shear stresses distributed over the length of an arbitrary fiber of length $l_f$, radius $r_f$, density $\rho_f$, and tensile modulus $E_f$ within a tensioned yarn once the fiber strain is known. These equations can be used to describe the radial distributions of the stresses in a yarn. For a fiber with helix angle $\theta$ in a yarn, according to the $\cos^2\theta$ law, we have the relationship between the yarn strain $\epsilon_y$ and the strain of the fiber $\epsilon_f$, including Poisson's effect:

$$\epsilon_f = \epsilon_y(\cos^2\theta - \nu_{LT}\sin^2\theta) \quad , \qquad (6)$$

where $\nu_{LT}$ is the yarn Poisson's ratio governing induced transverse strains due to longitudinal deformation, and was derived in Part I as

$$\nu_{LT} = \frac{M_{LT}{}^a K_L}{M_{LL}{}^a K_T} \quad . \qquad (7)$$

Assume $R_y$ as the radius of the yarn and $r$ the radial position in the yarn. Equation 6 can be expressed in terms of the relative radial position in the yarn $\frac{r}{R_y}$ according to [5]

$$\epsilon_f = \epsilon_y\left[\frac{c^2}{u^2} - \nu_{LT}\left(1 - \frac{c^2}{u^2}\right)\right] \quad , \qquad (8)$$

where $c^2 = \cos^2 q$ and

$$u^2 = \frac{r}{R_y}(1 - c^2) + c^2 \quad . \qquad (9)$$

To illustrate the stress distributions in the yarn, we can either use the results for the nonslipping case in Part I or, more reasonably, the results of the slipping case in Part II. For simplicity, however, we show only the former case here. In addition, because we demonstrated in Part I that these stresses are not constant over a fiber length, we will deal only with their maximum values. Bringing $\epsilon_f$ in Equation 8 into Equations 28 and 29 in Part I gives the maximum values of the tensile stress,

$$\sigma_{max} = E_f\epsilon_y\left[\frac{c^2}{u^2} - \nu_{LT}\left(1 - \frac{c^2}{u^2}\right)\right] \times\left[1 - \frac{1}{\cosh(ns)}\right] \quad , \qquad (10)$$

and the lateral pressure,

$$g_{max} = \frac{n}{2\mu}E_f\epsilon_y \times\left[\frac{c^2}{u^2} - \nu_{LT}\left(1 - \frac{c^2}{u^2}\right)\right]\tanh(ns) \quad , \qquad (11)$$

where $s = \frac{l_f}{2r_f}$ is the so-called fiber aspect ratio and $n$ is the yarn cohesion factor defined in Part I. Both $n$ and $\nu_{LT}$ are the functions of the yarn twist factor $T_y$, and their values at different twist levels were provided in Part I.

Furthermore, we can define the relative stresses to eliminate the yarn strain effect:

$$\sigma_y = \frac{\sigma_{max}}{E_f\epsilon_y} = \left[\frac{c^2}{u^2} - \nu_{LT}\left(1 - \frac{c^2}{u^2}\right)\right]\left[1 - \frac{1}{\cosh(ns)}\right] \qquad (12)$$

and

$$g_y = \frac{g_{max}}{E_f\epsilon_y} = \frac{n}{2\mu}\left[\frac{c^2}{u^2} - \nu_{LT}\left(1 - \frac{c^2}{u^2}\right)\right]\tanh(ns) \quad . \qquad (13)$$

Figures 2 and 3 depict the radial distributions of both stresses as well as the effect of the yarn twist factor. When yarn twist level is low, both tensile and lateral stresses are very small, and there is little variation of these stresses throughout the yarn cross section. When yarn twist level becomes high enough, both stresses possess the maximum values as determined by the yarn strain at the yarn center and decrease toward the yarn surface, a conclusion similar to the filament yarn case [5]. The data we used for the calculation are the same as in Parts I and II and are provided in Table I.

## Fiber Bending Effect on Yarn Properties

As we indicated in Part I of this series, when a yarn is under longitudinal tensile stress $\sigma_L$, fibers will ex-

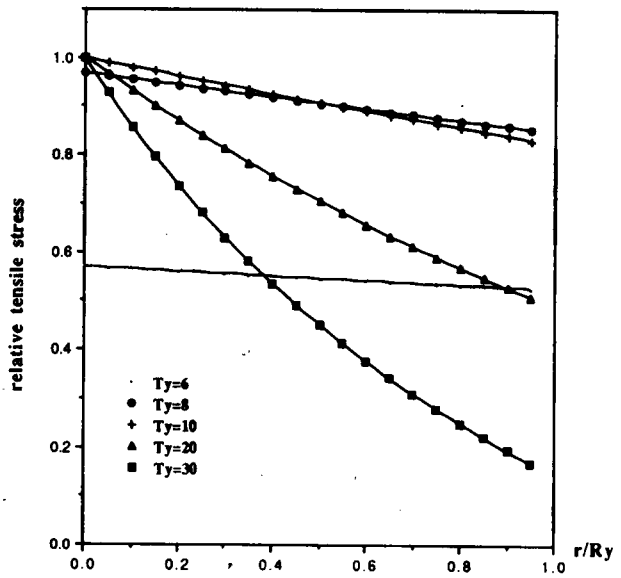


FIGURE 2. Radial distribution of relative tensile stress over a yarn cross section.

TABLE I. The fiber matrix properties used for calculation.

| Item | Typical value | Unit |
|---|---|---|
| Fiber radius $r_f$ | $3 \times 10^{-3}$ | cm |
| Fiber length $l_f$ | 3.0 | cm |
| Fiber specific density $\rho_f$ | 1.31 (1310 kg/m$^3$)[a] | g/cm$^3$ |
| Fiber modulus $E_f$ | $6 \times 10^7$ (5.88 GPa)[a] | g/cm$^2$ |
| Fiber frictional coefficient $\mu$ | 0.3 | |
| Fiber aspect ratio $s = \frac{l_f}{2r_f}$ | 500 | |

[a] The values in SI units.

perience, besides axial extension, bending deformation as well, due to fiber misalignment. There is also torsional deformation. These additional kinds of deformation have more significant effects on yarn properties when yarn twist level is high. Again for simplicity, we only consider the combined effects of axial extension and bending deformation on the longitudinal tensile modulus of a yarn.

Overall yarn strain $\epsilon_L$ caused by this longitudinal yarn tensile stress consists of contributions from fiber tensile ($\epsilon_{La}$) and bending deformation ($\epsilon_{Lb}$), *i.e.*,

$$\epsilon_L = \epsilon_{La} + \epsilon_{Lb} \quad . \tag{14}$$

The yarn longitudinal tensile modulus is thus defined as

$$E_L = \frac{\sigma_L}{\epsilon_L} = \frac{\sigma_L}{\epsilon_{La} + \epsilon_{Lb}} = \frac{1}{\frac{1}{E_{La}} + \frac{1}{E_{Lb}}} \tag{15}$$

or

$$\frac{1}{E_L} = \frac{1}{E_{La}} + \frac{1}{E_{La}} \quad , \tag{16}$$

where

$$E_{La} = \frac{\sigma_L}{\epsilon_{La}} \tag{17}$$

and

$$E_{Lb} = \frac{\sigma_L}{\epsilon_{Lb}} \quad , \tag{18}$$

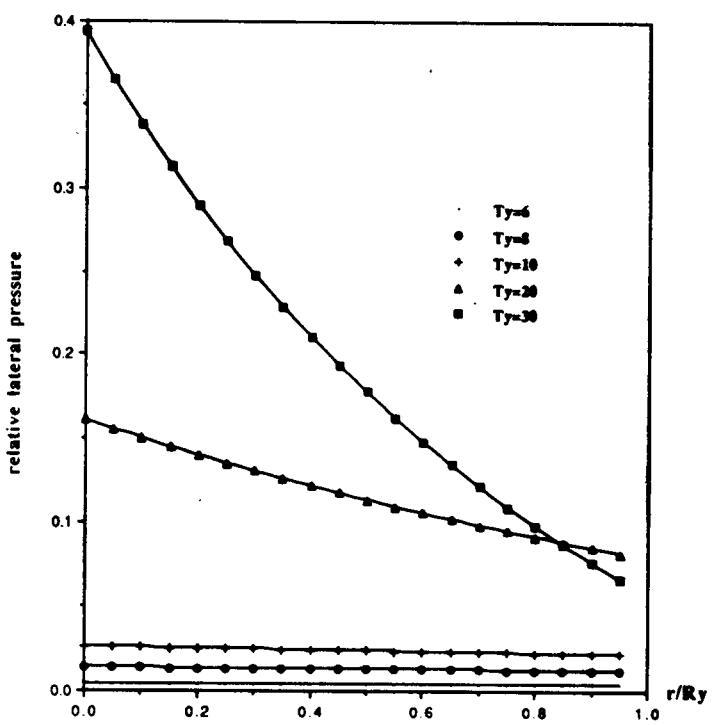


FIGURE 3. Radial distribution of relative lateral pressure over a yarn cross section.

corresponding to the tensile and bending components of the yarn modulus $E_L$, respectively.

Since Lee and Lee have analyzed the bending case for general fibrous assemblies [8], we use their results here to evaluate bending influence. According to Lee and Lee [8], when only fiber bending deformation is considered, the longitudinal modulus of a fibrous structure is given as

$$E_{Lb} = \frac{48 V_f^3 E_f K_L^2 I^2}{\pi^2 M_{LL}^b} \quad , \qquad (19)$$

where

$$I = \int_0^q d\theta \int_0^\pi d\phi J(\theta, \phi)\Omega(\theta, \phi) \sin\theta \qquad (20)$$

and

$$J(\theta, \phi) = \int_0^q d\theta' \int_0^\pi d\phi' \Omega(\theta', \phi') \times \sin\theta' \{1 - [\cos\theta \cos\theta' + \sin\theta \sin\theta' \cos(\phi - \phi')]^2\}^{1/2} \qquad (21)$$

are factors that reflect the fiber orientation, and $M_{LL}^b$ is the statistical factor associated with fiber bending deformation in the longitudinal direction [8]. Note again that for a yarn structure, the upper limit for $\theta$ is $q$.

For a staple yarn, we can apply the density function $f_1$ in Equation 1 in the analysis. Because of the independence of this density function on both $\theta$ and $\phi$, the factor $J(\theta, \phi)$ becomes a constant for any $\theta$ and $\phi$ values. Thus from Equation 21

$$J(\theta, \phi) = J(0, 0) = \frac{q - \cos q \sin q}{2(1 - \cos q)} \quad , \qquad (22)$$

and from Equation 20, we have

$$I = J(0, 0) \quad . \qquad (23)$$

Also using the same density function, we can calculate according to the expression for $M_{LL}^b$ [8],

$$M_{LL}^b = \frac{(\frac{2}{3} - \cos q + \frac{1}{3}\cos^3 q)}{(1 - \cos q)} \quad . \qquad (24)$$

Substituting $K_L = \frac{(1 + \cos q)}{2}$ already calculated in Part I and $M_{LL}^b$ into Equation 19 will give us the final expression for $E_{Lb}$:

$$E_{Lb} = \frac{3 V_f^3 E_f}{\pi^2} \times \frac{(q - \cos q \sin q)^2 (1 + \cos q)^2}{(\frac{2}{3} - \cos q + \frac{1}{3}\cos^2 q)(1 - \cos q)} \quad . \qquad (25)$$

Note that in Lee and Lee's analysis [8], they dealt with a bending case with concentrated loads at both ends of a fiber beam. We can certainly consider a case of distributed bending stress along the fiber length and modify the result above so as to include the fiber length effect, similar to the tensile case tackled in Part I. However, since fiber tensile breakage is the dominant, if not the only, form of fiber failure within the yarn, the distribution of bending stress along fiber length is therefore less significant and negligible.

In Part I, Equation 85, using the density function $f_1$, we already obtained the modulus component due to fiber axial tensile deformation:

$$E_{La} = \frac{3 V_f E_f \eta_l}{4} \frac{(1 + \cos q)^2}{1 + \cos q + \cos^2 q} \quad . \qquad (26)$$

The relationship between the yarn surface helix angle $q$ and the twist factor $T_y$ is provided in Equation 92 of Part I.

Let us now examine the effect of fiber bending deformation on yarn behavior. First of all, when there is no twist at all, fibers are all straight and aligned with the yarn axis, and the fiber helix angle equals to zero. As a result, fiber bending deformation due to yarn tension is zero. On the other hand, when twist is nonexistent in the staple yarn, the nominal tensile deformation is very large because fibers are sliding over each other with almost no resistance. Correspondingly, we can prove from the equations above that when twist factor $T_y = 0$, the bending component $E_{Lb}$ approaches infinity, whereas the tensile component $E_{La}$ equals zero. The overall yarn modulus $E_L$ is also zero.

Figures 4 and 5 show the predicted results in a relative scale using the ratio of yarn moduli and $E_f$, when the yarn twist factor begins to increase from $T_y = 1$. Figure 4, which compares the tensile and bending components of the yarn overall longitudinal modulus, shows that when the yarn twist factor is low, the bending component is much greater than the tensile component. In other words, yarn deformation under extension is more likely due to fiber tensile elongation than to fiber bending deformation. At high yarn twist levels, however, the bending component of the yarn modulus reaches the same level as the tensile component, so both contribute equally to yarn deformation. In addition, the fiber obliquity effect is reflected more significantly by bending than by the tensile component. Note that besides the surface helix angle $q$, the fiber volume fraction $V_f$ and the length efficiency factor associated with fiber tensile deformation $\eta_l$ are also functions of the yarn twist factor $T_y$.

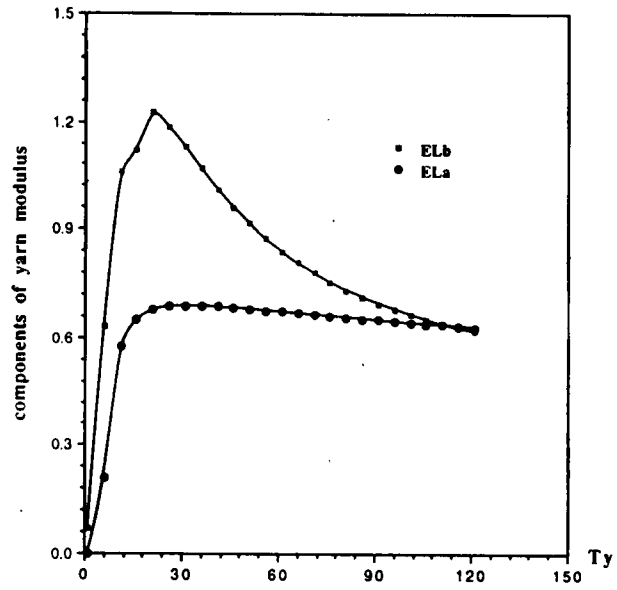


FIGURE 4. Two components of relative yarn longitudinal tensile modulus versus yarn twist factor.

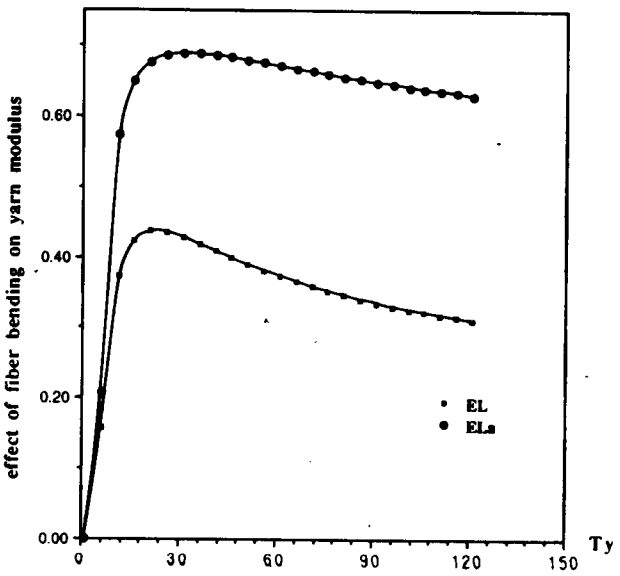


FIGURE 5. Comparison of relative yarn longitudinal tensile modulus with and without fiber bending effect.

Figure 5 provides two curves: curve $E_L$ is depicted based on Equation 15, in which both fiber tensile and bending deformation are considered. Curve $E_{La}$, based on Equation 26, contains the tensile component only. Again, when the yarn twist factor is small, the two curves are almost identical, conforming to the fact that at low twist level, yarn behavior is largely determined by fiber tensile deformation, and fiber bending deformation is too small to affect the result. However, as the yarn twist factor increases, the effect of fiber bending deformation becomes more significant. This effect reduces the yarn modulus and eventually the yarn tensile strength. From the results, we may also conclude that the fiber obliquity effect at high twist can be attributed more to fiber bending deformation.

## A Modified Model

We must admit that the fiber obliquity effect in yarn longitudinal tensile modulus as predicted by our method is still not entirely satisfactory, even when we include the bending mechanism. If our primary concern is to develop a model by which the experimental data can be most closely approximated, we can further modify the results above to establish a model yielding better predictions. We have suggested in Figure 1 that a more satisfactory result can be obtained by replacing $\theta$ with $2\theta$ into $\frac{K_L^2}{M_{LL}^a}$ for both density functions $f_1$ and $f_2$, but this will make the yarn surface helix angle exceed the 70.5 degree limit. Even though this limit may be different for staple yarn, as we assumed in Part I, the deviation is unlikely to be very large. Nevertheless, we can avoid this problem by defining an effective yarn surface helix angle $q_e$ for staple yarn as

$$q_e = 2 * q_t \quad , \tag{27}$$

where $q_t$ is the helix angle defined by Hearle [5] for filament yarns:

$$q_t = \arctan\left[10^{-3} T_y \left(\frac{40\pi}{\rho_f V_f}\right)\right] \quad . \tag{28}$$

Therefore we assume here that $q_t$ is the yarn surface helix angle for a filament yarn and is also the nominal surface helix angle for a staple yarn. But the actual effect of this helix angle has to be measured by $q_e$ due to the structural differences between the two yarn types.

Taking this effective yarn surface helix angle $q_e$ into Equation 15 will result in a modified model for predicting the longitudinal tensile modulus $E_L$ of the yarn. As shown in Figure 6, curve 1 represents the prediction using the old model as presented in Figure 5 (curve $E_L$). There the yarn surface helix is calculated according to Equation 92 in Part I,

$$q = \arctan\left[a_q 10^{-3} T_y \left(\frac{40\pi}{\rho_f V_f}\right)\right] \quad , \tag{29}$$

where $a_q = 2.5$ is a constant we used in Part I to account for the structural differences between the continuous

filament yarn and the staple yarn. Curve 2 is the prediction of the modified equation. Both results include the effect of fiber bending deformation.

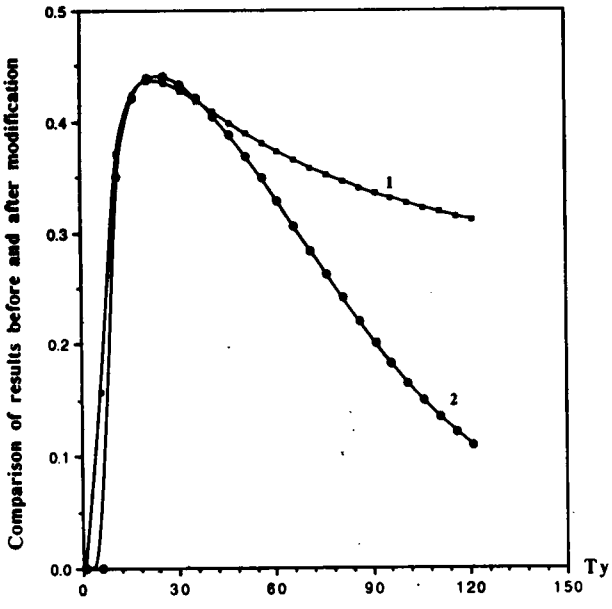


FIGURE 6. Prediction by the modified model in comparison with the original result.

Figure 6 shows that a slight difference exists between the two curves at a low twist level. At a high twist level, however, a fiber obliquity effect very close to the expected result is predicted by the modified model.

## Conclusions

In this study, we have shown that radial stress distributions within a staple yarn can be predicted using our theory. When yarn twist level is relatively high, the radial distributions of both tensile stress and lateral pressure over the yarn cross section are similar to the results of continuous filament yarn predicted in reference 5. At low twist level, however, both forces are lower than that determined by yarn strain, and also there are much smaller variations of them along the yarn cross section. Fiber bending deformation has a more significant effect on yarn properties at high twist levels. At lower twist levels, yarn properties are determined mainly by the tensile deformation of the constituent fibers.

The fiber obliquity effect is a complex phenomenon and depends on many factors such as the yarn fiber-volume fraction, the fiber orientation (the density function), and the kinds of fiber deformation involved. The modified model using a re-defined equation to calculate the yarn surface helix angle can closely predict this effect based on the physical, dimensional, and structural properties of the fibers and the yarn.

## Literature Cited

1. Carnaby, G. A., and Pan, N., Theory of the Compression Hysteresis of Fibrous Assemblies, *Textile Res. J.* **59**, 275 (1989).
2. Cox, H. L., The Elasticity and Strength of Paper and Other Fibrous Materials, *Br. J. Appl. Phys.* **3**, 72 (1952).
3. Corte, H., and Kallmes, O., Statistical Geometry of a Fibrous Network, in "Formation and Structure of Paper," vol. 1, F. Bolom, Ed., Tech. Sect. Brit. Papers and Board Makers Assoc., London, 1962, p. 13.
4. Gégauff, G., Force et elasticite des files en cotton, *Bull. Soc. Ind. Mulhouse* **77**, 153 (1907).
5. Hearle, J. W. S., Grosberg, P., and Backer, S., "Structural Mechanics of Yarns and Fabrics," vol. 1, Wiley-Interscience, NY, 1969, p. 180.
6. Kallmes, O., and Corte, H., The Structure of Paper: I, The Statistical Geometry of an Ideal Two-Dimensional Fiber Network, *TAPPI* **43**, 737 (1960).
7. Komori, T., and Makishima, K., Numbers of Fiber-to-Fiber Contacts in General Fiber Assemblies, *Textile Res. J.* **47**, 13–17 (1977).
8. Lee, D. H., and Lee, J. K., Initial Compressional Behavior of a Fiber Assembly, in "Objective Measurement: Applications to Product Design and Process Control," S. Kawabata, R. Postle, and M. Niwa, Eds., The Textile Machinery Society of Japan, Osaka, 1985, pp. 613.
9. Lee, D. H., and Lee, J. K., The Application of the Orientation Density Function to the Mechanics of a Fibrous Assembly, in "Proc. Advanced Workshop on Maths/Physics Application in the Wool Industry," Lincoln, New Zealand, 1988, p. 181.
10. Mardia, K. V., "Statistics of Directional Data," Academic Press, NY, 1972.
11. Pan, N., Development of a Constitutive Theory for Short Fiber Yarns: Mechanics of Staple Yarn Without Slippage Effect (Part I), *Textile Res. J.* **62**, 749–765 (1992).
12. Pan, N., Development of a Constitutive Theory for Short Fiber Yarns, Part II: Mechanics of Staple Yarn With Slippage Effect, *Textile Res. J.* **63**, 504–515 (1993).
13. Platt, M. M., Mechanics of Elastic Performance of Textile Materials, Part III: Some Aspects of Stress Analysis of Textile Structures—Continuous-Filament Yarns, *Textile Res. J.* **20**, 1 (1950).
14. Postle, R., Carnaby, G. A., and de Jong, S., "The Mechanics of Wool Structure," Ellis Horwood Limited, England, 1988.
15. van Wyk, C. M., Note on the Compressibility of Wool, *J. Textile Inst.* **37**, T285–292 (1946).
16. Zurek, W., "The Structure of Yarn," 2nd ed., WNT, Warsaw, Poland, 1975.

*Manuscript received June 22, 1992; accepted December 11, 1992.*